ELSEVIER

Contents lists available at ScienceDirect

# Journal of Environmental Chemical Engineering

journal homepage: www.elsevier.com/locate/jece



# New insights into the mechanism of azo dye biodegradation by *Lactococcus lactis*

Jean M.S. Oliveira a,b, Jan S. Poulsen b, Eugênio Foresti A, Jeppe L. Nielsen b,

- <sup>a</sup> Biological Processes Laboratory (LPB), São Carlos School of Engineering (EESC), University of São Paulo (USP), 1100 João Dagnone Avenue, São Carlos, SP 13563-120. Brazil
- b Center for Microbial Communities, Department of Chemistry and Bioscience, Aalborg University, Fredrik Bajers Vej 7H, Aalborg DK-9220, Denmark

#### ARTICLE INFO

#### Keywords:

Differential proteomics. Bioremediation. Glycoconjugates. Aromatic amines. Reductive decolorization

#### ABSTRACT

Azo dye reduction by syntrophic microbial communities is still unclear, with conflicting observations reported in the literature. In this study, the biodegradation mechanism of a model azo dye by *Lactococcus lactis* strain LLSP-01 isolated from an acidogenic reactor system was investigated. Proteomics and RT-PCR analysis results showed that LLSP-01 azoreductase (AzoL) was not expressed by the isolate during exposure to Direct Black 22. In contrast, the mechanism appears to involve biosorption by glycoconjugates, particularly exopolysaccharides (EPS) and rhamnolipids, as proteins from the LPS O-antigen metabolism were statistically higher expressed in cells challenged with the target compound. Based on the proteomic observations, it is hypothesized that Direct Black 22 is adsorbed into the biofilm matrix and indirectly reduced by an SDR family oxidoreductase, in a mechanism mediated by riboflavin carriers. Induction of a ring-cleaving dioxygenase in the presence of azo dye indicates further degradation of the resulting aromatic amines. The collected results show that azo dye reduction by *L. lactis* is mediated by enzymes with broad range specificity, and not the typical azoreductases. This information can assist in the design of new strategies for the bioremediation of textile azo dyes.

#### 1. Introduction

Biological degradation of azo dyes in wastewater reduces biotoxicity and has proven to be a safe and more cost-effective alternative to physico-chemical methods [2,8,30]. In reduced environments, azo dye is biodegraded cometabolically through a process termed *reductive decolorization*. This mechanism has been speculated to involve a reaction in which reducing equivalents, as well as reduced cofactors, work as secondary electron donors to cleave the azo bonds [35]. Moreover, a self-redox mechanism of azo dye degradation mediated by novel decolorizing hydrolases was recently proposed, adding complexity to the study of azo dye bioremediation [44].

Reductive decolorization in anaerobic reactors has been found to be correlated with the conversion of carbohydrates into volatile organic acids, organic solvents, and with hydrogen-producing pathways [31]. It can therefore be speculated whether enzymes involved in the carbohydrate metabolism catalyze the reductive cleavage of the azo bonds instead of the typical azoreductases. While azoreductases are more frequently found in aerobic bacteria, with few reports among strict anaerobes [26,28], it remains unclear if reductive decolorization by

syntrophic microbial communities happens mainly through the action of these specific enzymes in anoxic or anaerobic environments.

The advancement of molecular techniques has brought new life into the study of aromatic hydrocarbons' biodegradation, and proteomics approaches appear particularly useful for the identification and characterization of novel enzymes involved in the degradation pathway of such compounds [22]. Xenobiotics-degrading cells grown in the presence of the target compound induce expression of enzymes related to the catabolism of these compounds, and therefore these proteins can be identified through their differential abundance [1,21].

In this study, the degradation pathway of the azo dye Direct Black 22 (DB22) by *Lactococcus lactis* was investigated using a label-free proteomic approach. This bacterium, known for its diverse metabolic capabilities, especially in carbohydrate metabolism, was isolated from an acidogenic reactor system fed with synthetic textile wastewater and was significantly enriched throughout its operation [29]. The present research aims to explore whether enzymes involved in glycolytic and fermentative pathways play a role in the reductive cleavage of azo bonds, based on the correlation between carbohydrate metabolism and reductive decolorization observed in anaerobic reactors. Additionally,

E-mail address: jln@bio.aau.dk (J.L. Nielsen).

<sup>\*</sup> Corresponding author.

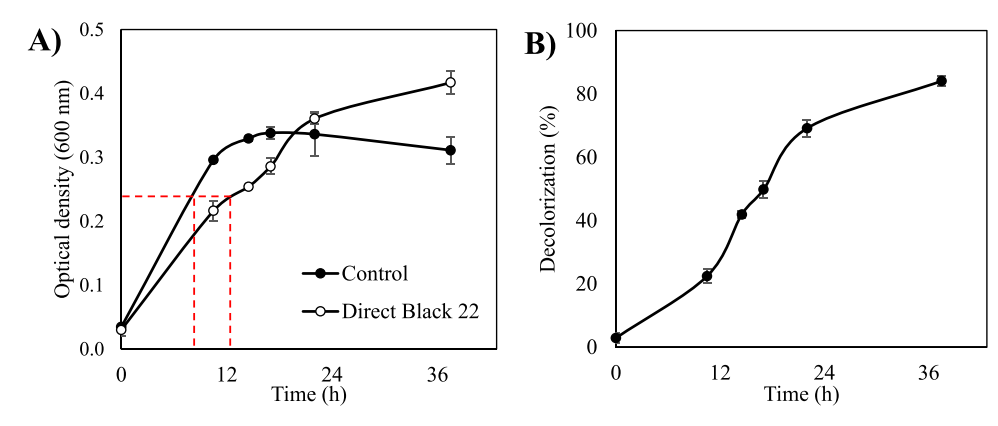
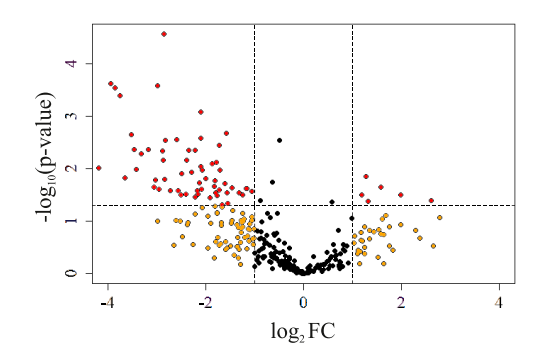


Fig. 1. Effects of the azo dye Direct Black 22 (DB22,  $32 \text{ mg} \cdot \text{L}^{-1}$ ) on the growth of *L. lactis* (A) and DB22 decolorization efficiency (B) over 38 h. Dashed lines represent the times during which samples were harvested for protein extraction. Assays were conducted in quadruplicates.



**Fig. 2.** Volcano plot generated to compare proteins differentially abundant in *L. lactis* LLSP-01 cells grown in the absence or presence of the azo dye Direct Black 22 (32  $\rm mg\cdot L^{-1}$ ). Vertical and horizontal dashed lines represent, respectively, the log fold change (log<sub>2</sub>FC) and p-value thresholds used to pronounce statistical significance.

we will investigate the presence of self-redox mechanisms mediated by novel decolorizing hydrolases [44], adding complexity to our understanding of azo dye degradation.

The findings provide novel information on the biodegradation of textile azo dyes by *Lactococcus lactis*, potentially revealing new enzymatic mechanisms beyond the well-characterized azoreductases. This can help in the design of more effective and sustainable bioremediation strategies, enhancing the application of syntrophic microbial communities in wastewater treatment processes.

#### 2. Materials and methods

# 2.1. Azo dye and synthetic textile wastewater

Direct Black 22 (DB22, CAS 6473–13–8, Aupicor Quimica©, Pomerode, Brazil) has a molecular weight of  $1084~g\cdot mol^{-1}$ , and the obtained compound had a purity of 42 %. The dye was hydrolyzed by increasing pH to 11 and heating at 80 °C for 1 h to simulate the actual state of the dye in textile effluents [36]. The basal medium used in the study was based on the composition of a real textile wastewater [3] and contained: DB22 (32.5 mg·L $^{-1}$ ), glucose (1.70 gCOD·L $^{-1}$ ), KH<sub>2</sub>PO<sub>4</sub> (0.25 g·L $^{-1}$ ), Na<sub>2</sub>SO<sub>4</sub> (0.50 g·L $^{-1}$ ), NaCl (0.50 g·L $^{-1}$ ), yeast extract (0.40 g·L $^{-1}$ ), NaHCO<sub>3</sub> (0.15 g·g $^{-1}$  COD), and 1 mL·L $^{-1}$  trace elements solution (supplementary material).

#### 2.2. Anaerobic bacterium isolation

A bacterium capable of decolorizing DB22 was isolated an aerobically from a continuous acidogenic reactor operated with synthetic textile

**Table 1** The top 15 proteins differientally abundant in *L. lactis* LLSP-01 cells grown in the presence of 32.5 mg·L $^{-1}$  Direct Black 22. Proteins with high abundance identified in the samples exposed to Direct Black 22 were also included.

p-value	$log_2FC$	Accession	Protein name or description
I — Upreg	ulated		
8.5E-02	2.78	WP_058211938.1	L-arabinose isomerase
4.0E-02	2.60	WP_046781838.1	WxL domain-containing protein
3.1E-02	1.99	WP_058217091.1	BMP family ABC transporter substrate- binding protein
2.2E-02	1.57	WP_058219886.1	SDR family oxidoreductase
4.2E - 02	1.31	WP_033899140.1	dTDP-glucose 4,6-dehydratase
1.4E-02	1.27	WP_064973379.1	ring-cleaving dioxygenase
3.1E-02	1.19	WP_003129660.1	vitamin B12 independent methionine synthase
-	-	WP_010905193.1	dTDP-4-dehydrorhamnose 3,5-epimerase
_	_	WP_058210984.1	phosphopyruvate hydratase
II — Down	regulated		
9.7E-03	-4.20	WP_004254538.1	DNA starvation/stationary phase protection
2.4E-04	-3.94	WP_058223384.1	aldo/keto reductase
2.9E-04	-3.86	WP_003129551.1	DNA-directed RNA polymerase subunit delta
4.3E-03	-3.47	WP_003129453.1	cell division regulator GpsB
1.0E-02	-3.42	WP_057720276.1	ammonia-dependent NAD(+) synthetase
4.3E-03	-3.18	WP_003130887.1	phosphate signaling complex protein PhoU
2.2E-02	-3.06	WP_081041499.1	5-bromo—4-chloroindolyl phosphate hydrolase
1.6E-02	-3.04	WP_038599155.1	FMN-dependent NADH-azoreductase
2.6E-04	-2.98	WP 003131560.1	superoxide dismutase [Mn]
4.7E-03	-2.89	WP 058219555.1	elongation factor Ts
6.9E-03	-2.87	WP_015426160.1	transcription regulator
2.7E-05	-2.87	WP_029344674.1	universal stress protein
1.6E-02	-2.84	WP_003130829.1	RNA polymerase sigma factor RpoD
2.8E-03	-2.83	WP 003131820.1	IreB family regulatory phosphoprotein

wastewater [29]. A serial dilution of the DB22-degrading consortium was applied in antibiotic flasks (50 mL) containing 25 mL of filter-sterilized basal medium. The flasks were flushed with  $N_2$  for 1 min and incubated at 30 °C under static conditions for a period of 48 h. The highest dilution that gave satisfactory color removal was plated on sterilized solid basal medium containing 1.5 % bacteriological agar. Petri dishes were incubated at 30 °C in a Gas-Pack jar with anaerobic sachets  $Oxoid^{TM}$  Anaero $Gen^{TM}$  (Thermo Fisher Scientific $^{TM}$ , Massachusetts, USA) for at least 24 h.

# 2.3. Decolorization assays

Decolorization assays were performed in quadruplicates using serum

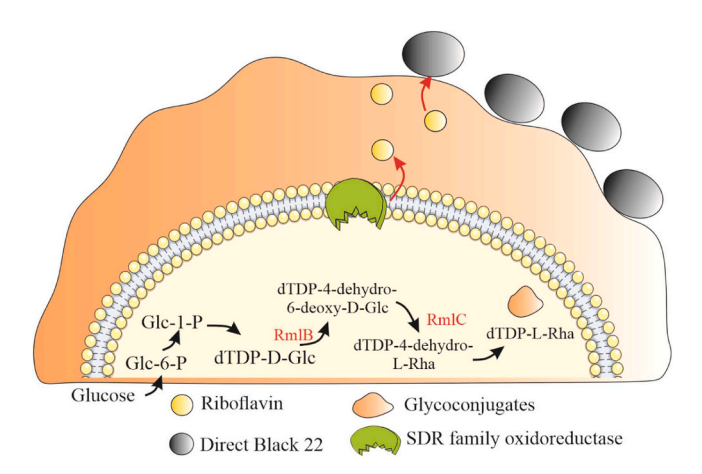


**Fig. 3.** Proposed biodegradation mechanism of the azo dye Direct Black 22by strain LLSP-01. RmlB (dTDP-glucose 4,6-dehydratase) and RmlC (dTDP-4-dehydrorhamnose 3,5-epimerase) were differentially more abundant in the presence of the azo dye. These enzymes are involved in the production of glycoconjugates in *L. lactis*, including rhamnose-containing exopolysaccharides and rhamnolipids. It is hypothesized that Direct Black 22 is adsorbed into the biofilm matrix and indirectly reduced by an SDR family oxidoreductase. Reducing equivalents are transferred through the extracellular matrix by hopping, in a mechanism mediated by riboflavin carriers.

bottles (250 mL) containing 100 mL of the basal medium. The flasks were inoculated with 10 % (vol/vol) cultures of *L. lactis* grown overnight and incubated at 30 °C with agitation at 150 rpm. Samples (1 mL) were periodically collected for color and optical density at 600 nm (OD<sub>600</sub>) measurements. Decolorization efficiency was calculated as indicated in the Eq. (1). Color interference on OD<sub>600</sub> measurements was eliminated by subtracting the absorbance values of centrifuged samples.

$$Decolorization = \frac{\int_{400nm}^{700nm} A_0.d\lambda - \int_{400nm}^{700nm} A_t.d\lambda}{\int_{400nm}^{700nm} A_0.d\lambda} . 100$$
 (1)

in which  $A_0$  is the initial absorbance of the sample;  $A_t$  is the absorbance of the sample at a time t; and  $d\lambda$  is an infinitesimal wavelength interval.

# 2.4. Whole-genome sequencing

# 2.4.1. High molecular weight DNA extraction

DNA was extracted using the DNeasy® Blood & Tissue Kit (Qiagen, Hilden, Germany) following the protocol of the manufacturer. DNA quantity was verified using a Qubit 2.0 fluorometer (Thermo Fisher Scientific, USA) with Qubit dsDNA BR Assay kit (Thermo Fischer Scientific, USA). DNA integrity was evaluated using a TapeStation 2200 with genomic DNA ScreenTapes (Agilent, USA).

# 2.4.2. Genome sequencing

DNA repair, end preparation, and ligation of sequencing adaptors were performed using the Native barcoding genomic DNA protocol in conjunction with the Ligation Sequencing Kit (MinION; Oxford Nanopore Technologies). The DNA library was loaded onto a MinION R9.4.1 flow cell and sequenced for 72 h using MinKNOW on a computer [37].

#### 2.4.3. Bioinformatics

Base calling was performed with Guppy v3.2.10 (https://community.nanoporetech.com). Porechop v0.2.3 was used to remove sequencing adaptors and for the demultiplexing of Nanopore reads (https://github.com/rrwick/Porechop). The quality of the sequences was assessed using NanoPlot v1.24.0 [14]. Reads were filtered for length (>600 bp) and quality (Q-score >10) using NanoFilt v.2.6.0 [14], and long-read assembly was conducted with Canu v2.0 [23]. The consensus genome was constructed after two rounds of polishing with Racon v1.3.3

[41] and Medaka v1.0.1 (https://github.com/nanoporetech/medaka). Genome assembly and completeness were assessed using BUSCO (benchmarking universal single-copy orthologs) v5.0.0 [24].

#### 2.5. Proteomics analysis

#### 2.5.1. Protein extraction

Bacterial cultures grown until mid-logarithmic growth phase (OD $_{600}$  = 0.24) were harvested by centrifugation at 4000 xg for 8 min and rinsed with ultrapure water. Growth conditions were similar to those described earlier (Section 2.3). Cell pellets were treated with a protease inhibitor cocktail and resuspended in a mixture containing 385  $\mu$ L TEAB buffer (50 mM triethylammonium bicarbonate, 1 % (w/w) sodium deoxycholate, pH 8.0), and 385  $\mu$ L B-PER lysis buffer. Samples were transferred to Covaris® AFA milliTUBEs, and cells were disrupted using a Covaris® focused-ultrasonicator system (Woburn, Massachusetts, United States). Extracted proteins were quantified using the Qubit Protein BR Assay Kit.

# 2.5.2. Peptide analysis

A total of 100  $\mu g$  of proteins were transferred to Protein LoBind® tubes and precipitated using cold acetone. Peptide digestion and purification were conducted using the PreOmics® iST kit (Planegg, Germany) and following the manufacturer's protocol. Tryptic peptides were analyzed using liquid chromatography – electrospray ionization tandem mass spectrometry (LC-ESI-MS/MS) as described elsewhere [16].

#### 2.5.3. Bioinformatic processing

Protein identification and quantification were performed with MaxQuant v2.0.3.1 [12], using the Andromeda search engine with default settings [13]. The false discovery rate used was 1 %. Carbamidomethylation was set as fixed modification, whereas acetylation of protein N-termini and oxidation of methionine were set as variable modifications. Samples spectra were searched against the predicted proteome from L. lactis isolate LLSP-01. The MaxLFQ algorithm was used to quantify proteins with at least one unique or razor peptide. The protein groups and evidence files were inputted into MSstats for further statistical analysis [10]. Contaminants and peptide and charge with only one or two measurements across runs were removed. Data was optimized for statistical modelling using log-transformation with base 2 and quantile normalization to remove systematic bias between MS runs. Protein summarization was performed using the Tukey's median polish, and linear mixed effects model with Empirical Bayes moderation was used to compare the two conditions (control and DB22-exposed groups) for differentially abundant proteins [15].

# 2.6. RNA isolation and RT-PCR analysis

 $L.\ lactis\ LLSP-01$  was grown under identical conditions as described earlier for the proteomics analysis. Exponentially growing cells incubated without and with 32.5 mg·L $^{-1}$  DB22 were harvested by centrifugation at 4000 xg for 8 min. RNA extraction was conducted using the RNeasy® kit (Qiagen, Hilden, Germany) according to the protocol of the manufacturer. RNA quality was assessed using TapeStation 2200 with genomic RNA ScreenTape (Agilent, USA), and concentration was measured using Qubit 2.0 (Thermo Fisher Scientific, USA) with Qubit RNA BR Assay kit (Thermo Fischer Scientific, USA).

Complimentary DNA (cDNA) was synthetized by reverse transcription of total RNA (1  $\mu$ g) using the SuperScript<sup>TM</sup> III First-Strand Synthesis System (Thermo Fisher Scientific, USA). cDNA was amplified by PCR using *L. lactis* LLSP-01 azoreductase (AzoL) primers designed using the RealTime PCR Design Tool (Integrated DNA technologies, Coralville, USA). Primers used were AzoL-fw (5'-GGT CCT GTT GGT TTA GCA AAT G-3') and AzoL-rev (5'- GTC CTT CAA CGG CAA TTT GTC-3'). PCR settings were as follows: initial denaturation at 95 °C for 2 min; amplification for 25 cycles at 95 °C for 15 s, 58.6 °C for 15 s, and 72 °C for 20 s;

$$H_2N$$
 $H_2N$ 
 $H_2N$ 

Fig. 4. Partial degradation of Direct Black 22 reduction products by L. lactis LLSP-01. Aromatic products such as 2,4-triaminobenzene, oxalic acid p-phenylenediamine, and 2-aminobenzenesulfonate are converted to catecholic compounds, which have their aromatic rings cleaved by a ring-cleaving dioxygenase.

and a final extension of 5 min at 72 °C.

#### 3. Results and discussion

# 3.1. DB22 decolorization by L. lactis

 $\it L.\ lactis$  reached decolorization efficiencies of up to 84.1 % after incubation for 37 h at 30 °C (Fig. 1). Cells exposed to DB22 presented lower growth rates, suggesting that the azo dye had an inhibitory effect on  $\it L.\ lactis$ . However, cells grown under DB22-induced stress presented higher optical densities after 37 h (OD\_{600}=0.42\pm0.02, N=4), while non-exposed cells (control) reached the stationary phase earlier, after 17 h (OD\_{600}=0.34\pm0.01, N=4). It was hypothesized that the higher biomass yields achieved in the presence of DB22 resulted from the higher concentration of substrate in these experiments, as DB22 can serve as additional substrate to support  $\it L.\ lactis$  growth. However, this phenomenon could also be caused by metabolic changes induced by the azo dye. The physiological and metabolic responses of  $\it L.\ lactis$  challenged with DB22 were further investigated using label-free proteomics analysis.

### 3.2. Strain verification and genome quality

The whole genome of *L. lactis* was sequenced, generating a total of 1.1 M reads and 2.3 Gb. After filtering on quality and trimming, 265,205 reads remained and a total of 489.2 Mb, resulting in a coverage of 313. The estimated completeness of the genome was 97.6 % based on BUSCO analysis. An average nucleotide identity (ANI) analysis showed that the strain had a 97.8 % similarity with *Lactococcus lactis* IO-1 (AP012281).

# 3.3. Proteomics analysis of L. lactis challenged with the azo dye

A total of 9080 proteins were detected in the differential proteomics analysis, of which 68 significantly changed in abundance when L. lactis was exposed to 32.5 mg·L $^{-1}$  DB22 (p  $\leq$  0.05;  $log_2FC < -1$  or  $log_2FC > 1$ ). While 61 proteins were relatively less abundant, only 7 proteins increased in abundance upon growth in the presence of the azo dye, and two were detected only in the positive group (Fig. 2 and Table 1; for the full list of significantly expressed proteins, refer to the supplementary materials).

The experiment conducted with biological quadruplicates revealed a

change in the metabolic pathways favoring production of L-ribulose from L-arabinose, as L-arabinose isomerase had the highest increment in abundance in the presence of DB22 ( $\log_2 FC = 2.78$ ). L-Ribulose is a precursor of D-Ribulose 5-phosphate, which is related to the biosynthesis of riboflavin through the pentose phosphate pathway [18,19]. Riboflavin is a well-known redox mediator involved in the co-metabolic degradation of azo dyes [17]. This finding suggests that microbial strains with a high production of riboflavin could enhance the reduction of azo bonds, facilitating the biodegradation of these compounds in industrial wastewater treatment processes.

A SDR family oxidoreductase also had an increase in its abundance ( $\log_2 FC = 1.57$ ), compared to the control group. Short-chain dehydrogenases/reductases is a family of NADPH-dependent oxidoreductases [20], which has previously been shown to play a major role in decolorization of azo dyes [38]. This underscores the importance of these enzymes in the degradation process, suggesting that leveraging NADPH-dependent oxidoreductases in biodegradation technologies could improve the efficiency of azo dye removal from wastewater. Enhancing the activity or expression of these enzymes in microbial strains used in bioremediation could significantly advance the development of effective treatment methods for industrial effluents containing azo dyes.

Proteins involved in the LPS O-antigen metabolism were also more abundant in the proteomes of L. lactis, which had been exposed to the azo dye. dTDP-glucose 4,6-dehydratase (log<sub>2</sub>FC = 1.31) converts dTDP- $\alpha$ -D-glucose into dTDP-4-dehydro-6-deoxy- $\alpha$ -D-glucose, which is then converted into dTDP-4-dehydro-β-L-rhamnose in a reaction catalyzed by dTDP-4-dehydrorhamnose 3,5-epimerase (identified only in samples exposed to DB22) [25]. These proteins are involved in the production of both cell wall polysaccharides and rhamnose-containing EPS in L. lactis [6], which might be related to the higher OD yields observed in cells exposed to the azo dye. Additionally, the increased levels of these enzymes suggest that L. lactis may produce rhamnolipids in response to azo dye exposure. Rhamnolipids enhance the bioavailability of hydrophobic organic pollutants by reducing surface tension, thereby facilitating their uptake and degradation by microorganisms. This implies that the production of rhamnolipids in L. lactis could play a significant role in the biodegradation of azo dyes by improving the emulsification and subsequent degradation of these compounds.

A recent study showed that the decolorization of an azo dye by Aliiglaciecola lipolytica was initiated through dye adsorption into EPS. Increased production of EPS stimulates biosorption and flocculation, and the adsorbed dve was degraded through the action of oxidoreductases such as azoreductase and laccase [42]. Other studies have reported the relevant contribution of biofilm-mediated degradation in the bioremediation of xenobiotics by EPS-producing microor-[34]. dTDP-glucose 4,6-dehydratase dTDP-4-dehydro-β-L-rhamnose are also key enzymes involved in the biosynthesis of rhamnolipids, which are extracellular glycoconjugates that act as emulsifiers [11]. These biosurfactants play an important role in the bioremediation of organic pollutants, as they can reduce surface tension and therefore increase the bioavailability of these compounds [5]. The involvement of rhamnolipids is supported by previous reports showing their ability to promote the dissolution, biosorption, adsorption, and enhanced degradation of organic contaminants [5,27,45].

Moreover, L. lactis presented increased abundance of a WxL domain-containing protein ( $log_2FC=2.60$ ). The WxL region is a cell wall-biding domain, and therefore proteins fused to this domain are displayed on the bacterial surface [7]. Protein-displaying bacteria can act as bio-adsorbents [33], and we therefore hypothesize that L. lactis initiates DB22 decolorization through biosorption of the dye, enhancing the overall degradation process. The adsorption of DB22 to the cell surface proteins likely facilitates its initial capture and concentration, which may increase the efficiency of subsequent degradations steps. Following this, the reduction of the azo bonds is mediated by an SDR family oxidoreductase, with riboflavin acting as redox mediator.

Surprisingly, a ring-cleavage dioxygenase was also upregulated in the presence of DB22 ( $\log_2 FC = 1.27$ ). This enzyme catalyzes the ring fission of aromatic compounds such as benzene, naphthalene, and aromatic amines [40]. Moreover, ring-cleaving dioxygenases were found to be involved in the detoxification of direct azo dyes by a facultative anaerobe [9]. It is hypothesized that this enzyme contributed substantially to the biodegradation of DB22 in the initial stage of the experiment, *i.e.*, before oxygen was totally depleted. The upregulation of this enzyme suggests that microaerophilic conditions could be beneficial for the complete mineralization of azo dyes, as they enable both the reductive decolorization of azo bonds and the partial degradation of aromatic amines.

Several transcription regulators and proteins involved in the regulation of cell growth were statistically less abundant in the cells challenged with the azo dye. These proteins include cell division regulator GpsB (log<sub>2</sub>FC = -3.47), phosphate signaling complex protein PhoU (log<sub>2</sub>FC = -3.18), DNA-directed RNA polymerase subunit delta (log<sub>2</sub>FC = -3.86), transcription regulator (log<sub>2</sub>FC = -2.87), and RNA polymerase sigma factor RpoD (log<sub>2</sub>FC = -2.84). Proteins involved in the cellular process of translation (e.g., elongation factor Ts) were downregulated as well. These results support the decreased growth rates in *L. lactis* cells grown in the presence of DB22, showing that the azo dye and its biodegradation products induce several stress responses in *L. lactis*.

# 3.4. FMN-dependent NADH azoreductase not induced by the presence of DR22

Interestingly, an FMN-dependent NADH azoreductase, which catalyzes reductive cleavage of azo bonds [35], was identified with higher abundances in the control group ( $\log_2 FC = -3.04$ ). Morrison and John [28] observed azoreductase activity in extracts from the periplasmic fraction of *Clostridium perfringens* cells in both the dye- and the non-dye exposed group. The authors further showed that the charged groups on sulfonated dyes caused the release of azoreductase into the extracellular matrix, and that protein secretion was not caused by cell lysis or leakage. This resulted in increased azoreductase activity in extracts from the periplasmic fractions of cells not previously exposed to sulfonated azo dyes. It is therefore hypothesized that azoreductase was released upon exposure to DB22, therefore explaining the lower abundance of the enzyme within cells challenged with the dye.

To test this hypothesis, we searched for the genetic presence of signal peptides in the L. lactis LLSP-01 AzoL protein using the Signal P 6.0 prediction software [39]. However, no such signal peptides were found, suggesting that the AzoL are not translocated across the bacterial membrane. Further analysis using RT-PCR supported these findings, as no increase in AzoL amplicons was observed for the control group nor for cells exposed to lower (1  ${\rm mg} \cdot {\rm L}^{-1}$ ) or higher (32.5  ${\rm mg} \cdot {\rm L}^{-1}$ ) concentrations of DB22, while the band corresponding to AzoL was clearly observed in the genomic DNA of L. lactis (Supplementary materials). These results agree with the findings from the proteomic analysis. It was therefore hypothesized that AzoL is not continuously expressed during the growth of L. lactis, and this enzyme is not transcriptionally, nor translationally, regulated by the presence of DB22.

# 3.5. Direct Black 22 biodegradation mechanism

We have proposed a model for the biodegradation of DB22 by *L. lactis*, based on the differentially expressed proteins. Our findings suggest that the process begins with the dye adsorbing to the biofilm matrix, as LLSP-01 synthesize glycoconjugates in the presence of the azo compound (Fig. 3). Production of EPS and rhamnolipids was induced as revealed by the increased levels of two enzymes involved in the LPS O-antigen metabolism, *i.e.*, dTDP-glucose 4,6-dehydratase (RmlB) and dTDP-4-dehydrorhamnose 3,5-epimerase (RmlC). The adsorbed dye is indirectly reduced by a NAD(P)H-dependent SDR family

oxidoreductase. Electrons produced in the interior of the cells are carried through the biofilm matrix by hopping, in a mechanism mediated by riboflavin carriers. Hopping has previously been shown as the prevailing pathway for extracellular electron transfer across EPS matrices [43].

Reductive cleavage of the azo bonds yields monocyclic aromatic amines such as 1,2,4-triaminobenzene, oxalic acid p-phenylenediamine, and 2-aminobenzenesulfonate. These molecules can be converted to catechol derivatives and to 3-sulfocatechol (Fig. 4), in reactions catalyzed by aniline dioxygenase [4,32]. Further degradation by ring-cleaving dioxygenases [40] results in the formation of compounds with the skeleton of the 2-aminomuconic acid and 3-sulfomuconate.

Ring-cleaving dioxygenases activates molecular oxygen to form complex with the substrate molecule leading to the formation of a highly reactive intermediate, which undergoes rearrangements facilitated by the enzyme, resulting in the formation of two products [40]. *L. lactis* is a facultative anaerobe isolated from a continuous acidogenic reactor system. In the bioreactor system, the textile effluent was pumped at a high flow rate, and the feed tank was not flushed with nitrogen to strip the oxygen. It was hypothesized that the wastewater contained dissolved oxygen that could serve as substrate for the ring-cleaving dioxygenase enzyme immediately upon entrance in the reactor. To simulate the same conditions, nitrogen was not flushed in the flasks during the proteomics experiment with *L. lactis*, and DB22 products were partially degraded before the complete depletion of oxygen in the flasks.

Our findings align with previous reports on biosorption as the initial stage in the biodegradation of structurally similar azo dyes [46]. Notably, our study stands out as the first to highlight that proteins involved in the LPS O-antigen metabolism were more abundant in L. lactis exposed to DB22, indicating enhanced EPS production. EPS can promote dye adsorption and self-flocculation, which are critical initial steps in the biodegradation process. The role of EPS in facilitating biosorption and providing a matrix for subsequent enzymatic degradation highlights a potential strategy for biofilm-based treatment systems. This approach could be particularly useful in bioreactors designed for azo dye-containing effluents, where initial adsorption followed by enzymatic reduction can efficiently degrade the dyes. Furthermore, the engagement of ring-cleaving dioxygenases under low oxygen concentrations provides valuable insights for designing wastewater treatment technologies. Microaerophilic conditions appear beneficial, enabling both the reductive decolorization of azo bonds and the partial degradation of aromatic amines.

# 4. Conclusion

Biosorption plays an important role in the biodegradation of azo dyes by *L. lactis*, and the reduction mechanism initiates with adsorption of the dye to the biofilm matrix. The adsorbed dye is reduced by an SDR family oxidoreductase, showing that enzymes with broad range specificity are involved. Reducing equivalents are transferred through the biofilm matrix until the azo compound by hopping, in a mechanism mediated by riboflavin. Resulting aromatic amines are partially degraded, while oxygen is still present in reactions catalyzed by a ring-cleaving dioxygenase. This challenges the conventional role of azoreductases, offering valuable insights for textile azo dye bioremediation strategies.

# CRediT authorship contribution statement

Jan S. Poulsen: Software, Formal analysis, Data curation. Jean M. S. Oliveira: Writing – original draft, Methodology, Investigation, Formal analysis, Data curation. Jeppe Lund Nielsen: Writing – review & editing, Supervision, Resources, Project administration, Funding acquisition, Conceptualization. Eugênio Foresti: Resources, Project administration, Funding acquisition, Conceptualization.

#### **Declaration of Competing Interest**

The authors declare that they have no known competing financial interests or personal relationships that could have appeared to influence the work reported in this paper.

#### **Data Availability**

Data will be made available on request.

#### Acknowledgements

This work was supported by Aalborg University, the Fundação do Amparo à Pesquisa do Estado de São Paulo (process numbers 2015/06246-7, 2018/24269-2 and 2020/11860-4) and the Coordenação de Aperfeiçoamento de Pessoal de Nível Superior (CAPES) – Brazil (Finance Code001). The authors also would like to thank Dr. Nadieh de Jonge for her technical support.

# Appendix A. Supporting information

Supplementary data associated with this article can be found in the online version at doi:10.1016/j.jece.2024.113670.

#### References

- [1] B. Almeida, H. Kjeldal, I. Lolas, A.D. Knudsen, G. Carvalho, K.L. Nielsen, M. T. Barreto Crespo, A. Stensballe, J.L. Nielsen, Quantitative proteomic analysis of ibuprofen-degrading Patulibacter sp. strain I11, Biodegradation 24 (2013) 615–630, https://doi.org/10.1007/s10532-012-9610-5.
- [2] F.M. Amaral, M.T. Kato, L. Florêncio, S. Gavazza, Color, organic matter and sulfate removal from textile effluents by anaerobic and aerobic processes, Bioresour. Technol. 163 (2014) 364–369, https://doi.org/10.1016/j.biortech.2014.04.026.
- [3] S.M. Amorim, M.T. Kato, L. Florencio, S. Gavazza, Influence of redox mediators and electron donors on the anaerobic removal of color and chemical oxygen demand from textile effluent, Clean. - Soil, Air, Water 41 (2013) 928–933, https://doi.org/ 10.1002/clen.201200070.
- [4] P.K. Arora, Bacterial degradation of monocyclic aromatic amine. Front. Microbiol. 6 (2015) 1–14, https://doi.org/10.3389/fmicb.2015.00820.
- [5] P. Bhatt, A. Verma, S. Gangola, G. Bhandari, S. Chen, Microbial glycoconjugates in organic pollutant bioremediation: recent advances and applications, Microb. Cell Fact. 20 (2021) 1–18, https://doi.org/10.1186/s12934-021-01556-9.
- [6] I.C. Boels, M.M. Beerthuyzen, M.H.W. Kosters, M.P.W. Van Kaauwen, M. Kleerebezem, W.M. De Vos, Identification and functional characterization of the Lactococcus lactis rfb operon, required for dTDP-rhamnose biosynthesis, J. Bacteriol. 186 (2004) 1239–1248, https://doi.org/10.1128/JB.186.5.1239-1248.2004.
- [7] S. Brinster, S. Furlan, P. Serror, C-terminal WxL domain mediates cell wall binding in Enterococcus faecalis and other gram-positive bacteria, J. Bacteriol. 189 (2007) 1244–1253. https://doi.org/10.1128/JB.00773-06.
- [8] J.R.S. Carvalho, F.M. Amaral, L. Florencio, M.T. Kato, T.P. Delforno, S. Gavazza, Microaerated UASB reactor treating textile wastewater: the core microbiome and removal of azo dye Direct Black 22, Chemosphere 242 (2020) 125157, https://doi. org/10.1016/j.chemosphere.2019.125157.
- [9] G. Chen, X. An, H. Li, F. Lai, E. Yuan, X. Xia, Q. Zhang, Detoxification of azo dye Direct Black G by thermophilic Anoxybacillus sp. PDR2 and its application potential in bioremediation, Ecotoxicol. Environ. Saf. 214 (2021) 112084, https://doi.org/10.1016/j.ecoenv.2021.112084.
- [10] M. Choi, C.-Y. Chang, T. Clough, D. Broudy, T. Killeen, B. MacLean, O. Vitek, MSstats: an R package for statistical analysis of quantitative mass spectrometrybased proteomic experiments, Bioinformatics 30 (2014) 2524–2526, https://doi. org/10.1093/bioinformatics/btu305.
- [11] H. Chong, Q. Li, Microbial production of rhamnolipids: Opportunities, challenges and strategies, Microb. Cell Fact. 16 (2017) 1–12, https://doi.org/10.1186/ s12934-017-0753-2
- [12] J. Cox, M. Mann, MaxQuant enables high peptide identification rates, individualized p.p.b.-range mass accuracies and proteome-wide protein quantification, Nat. Biotechnol. 26 (2008) 1367–1372, https://doi.org/10.1038/ nbt.1511.
- [13] J. Cox, N. Neuhauser, A. Michalski, R.A. Scheltema, J.V. Olsen, M. Mann, Andromeda: a peptide search engine integrated into the MaxQuant environment, J. Proteome Res. 10 (2011) 1794–1805, https://doi.org/10.1021/pr101065j.
- [14] W. De Coster, S. D'Hert, D.T. Schultz, M. Cruts, C. Van Broeckhoven, NanoPack: visualizing and processing long-read sequencing data, Bioinformatics 34 (2018) 2666–2669, https://doi.org/10.1093/bioinformatics/bty149.
- [15] Föll, M., Fahrner, M., 2022. MaxQuant and MSstats for the analysis of label-free data (Galaxy Training Materials) [WWW Document]. URL <a href="https://training.galax">https://training.galax</a>

- yproject.org/training-material/topics/proteomics/tutorials/maxquant-msstats-dda-lfq/tutorial.html) (accessed 5.8.22).
- [16] P.J. García-Moreno, S. Gregersen, E.R. Nedamani, T.H. Olsen, P. Marcatili, M. T. Overgaard, M.L. Andersen, E.B. Hansen, C. Jacobsen, Identification of emulsifier potato peptides by bioinformatics: application to omega-3 delivery emulsions and release from potato industry side streams, Sci. Rep. 10 (2020) 690, https://doi.org/10.1038/s41598-019-57229-6
- [17] M. Imran, M. Arshad, F. Negm, A. Khalid, B. Shaharoona, S. Hussain, S. Mahmood Nadeem, D.E. Crowley, Yeast extract promotes decolorization of azo dyes by stimulating azoreductase activity in Shewanella sp. strain IFN4, Ecotoxicol. Environ. Saf. 124 (2016) 42–49, https://doi.org/10.1016/j.ecoenv.2015.09.041.
- [18] M. Kanehisa, KEGG: Kyoto encyclopedia of genes and genomes, Nucleic Acids Res 28 (2000) 27–30, https://doi.org/10.1093/nar/28.1.27.
- [19] M. Kanehisa, M. Araki, S. Goto, M. Hattori, M. Hirakawa, M. Itoh, T. Katayama, S. Kawashima, S. Okuda, T. Tokimatsu, Y. Yamanishi, KEGG for linking genomes to life and the environment, Nucleic Acids Res. 36 (2008) 480–484, https://doi.org/ 10.1093/nar/gkm882.
- [20] K.L. Kavanagh, H. Jörnvall, B. Persson, U. Oppermann, Medium- and short-chain dehydrogenase/reductase gene and protein families: the SDR superfamily: Functional and structural diversity within a family of metabolic and regulatory enzymes, Cell. Mol. Life Sci. 65 (2008) 3895–3906, https://doi.org/10.1007/ s00018-008-8588-y.
- [21] S.-J. Kim, R.C. Jones, C.-J. Cha, O. Kweon, R.D. Edmondson, C.E. Cerniglia, Identification of proteins induced by polycyclic aromatic hydrocarbon in Mycobacterium vanbaalenii PYR-1 using two-dimensional polyacrylamide gel electrophoresis andde novo sequencing methods, Proteomics 4 (2004) 3899–3908, https://doi.org/10.1002/pmic.200400872.
- [22] S.J. Kim, O. Kweon, C.E. Cerniglia, Proteomic applications to elucidate bacterial aromatic hydrocarbon metabolic pathways, Curr. Opin. Microbiol. 12 (2009) 301–309, https://doi.org/10.1016/j.mib.2009.03.006.
- [23] S. Koren, B.P. Walenz, K. Berlin, J.R. Miller, N.H. Bergman, A.M. Phillippy, Canu: scalable and accurate long-read assembly via adaptive k-mer weighting and repeat separation, Genome Res 27 (2017) 722–736, https://doi.org/10.1101/ or 215087 116
- [24] M. Manni, M.R. Berkeley, M. Seppey, F.A. Simão, E.M. Zdobnov, BUSCO Update: novel and streamlined workflows along with broader and deeper phylogenetic coverage for scoring of eukaryotic, prokaryotic, and viral genomes, Mol. Biol. Evol. (2021) 1–8. https://doi.org/10.1093/molbey/msab199.
- [25] C.L. Marolda, M.A. Valvano, Genetic analysis of the dTDP-rhamnose biosynthesis region of the Escherichia coli VW187 (O7:K1) rfb gene cluster: identification of functional homologs of rfbB and rfbA in the rff cluster and correct location of the rffE gene, J. Bacteriol. 177 (1995) 5539–5546, https://doi.org/10.1128/ ib.177.19.5539-5546.1995.
- [26] S.A. Misal, K.R. Gawai, Azoreductase: a key player of xenobiotic metabolism, Bioresour. Bioprocess. 5 (2018), https://doi.org/10.1186/s40643-018-0206-8.
- [27] I. Mnif, D. Ghribi, Glycolipid biosurfactants: main properties and potential applications in agriculture and food industry, J. Sci. Food Agric. 96 (2016) 4310–4320, https://doi.org/10.1002/jsfa.7759.
- [28] J.M. Morrison, G.H. John, Non-classical azoreductase secretion in Clostridium perfringens in response to sulfonated azo dye exposure, Anaerobe 34 (2015) 34–43, https://doi.org/10.1016/j.anaerobe.2015.04.007.
- [29] J.M.S. Oliveira, M.H.R.Z. Damianovic, E. Foresti, Two-stage anaerobic digestion system for biotransformation of an azo dye in the presence of sulfate: minimizing competition for reducing equivalents, J. Water Process Eng. 47 (2022) 102819, https://doi.org/10.1016/j.jwpe.2022.102819.
- [30] J.M.S. Oliveira, M.R. de Lima e Silva, C.G. Issa, J.J. Corbi, M.H.R.Z. Damianovic, E. Foresti, Intermittent aeration strategy for azo dye biodegradation: A suitable alternative to conventional biological treatments? J. Hazard. Mater. 385 (2020) 9, https://doi.org/10.1016/j.jhazmat.2019.121558.
- [31] J.M.S. Oliveira, J.S. Poulsen, E. Foresti, J.L. Nielsen, Microbial communities and metabolic pathways involved in reductive decolorization of an azo dye in a two-

- stage AD system, Chemosphere 310 (2023) 136731, https://doi.org/10.1016/j.chemosphere.2022.136731.
- [32] K. Perei, G. Rákhely, I. Kiss, B. Polyák, K.L. Kovács, Biodegradation of sulfanilic acid by Pseudomonas paucimobilis, Appl. Microbiol. Biotechnol. 55 (2001) 101–107, https://doi.org/10.1007/s002530000474.
- [33] T.V. Plavec, B. Štrukelj, A. Berlec, Screening for new surface anchoring domains for lactococcus lactis, Front. Microbiol. 10 (2019) 1–13, https://doi.org/10.3389/ fmicb.2019.01879.
- [34] N. Premnath, K. Mohanrasu, R. Guru Raj Rao, G.H. Dinesh, G.S. Prakash, V. Ananthi, K. Ponnuchamy, G. Muthusamy, A. Arun, A crucial review on polycyclic aromatic Hydrocarbons - environmental occurrence and strategies for microbial degradation, Chemosphere 280 (2021) 130608, https://doi.org/ 10.1016/j.chemosphere.2021.130608.
- [35] A.B. Santos, F.J. Cervantes, J.B. van Lier, Review paper on current technologies for decolourisation of textile wastewaters: perspectives for anaerobic biotechnology, Bioresour. Technol. 98 (2007) 2369–2385, https://doi.org/10.1016/j. biortech.2006.11.013.
- [36] A.B. Santos, F.J. Cervantes, J.B. Van Lier, Azo dye reduction by thermophilic anaerobic granular sludge, and the impact of the redox mediator anthraquinone-2,6-disulfonate (AQDS) on the reductive biochemical transformation, Appl. Microbiol. Biotechnol. 64 (2004) 62–69, https://doi.org/10.1007/s00253-003-1428-y.
- [37] M. Sereika, R.H. Kirkegaard, S.M. Karst, T. Yssing Michaelsen, E.A. Sørensen, R. D. Wollenberg, M. Albertsen, Oxford Nanopore R10.4 long-read sequencing enables the generation of near-finished bacterial genomes from pure cultures and metagenomes without short-read or reference polishing, Nat. Methods 19 (7) (2022) 823–826, https://doi.org/10.1038/s41592-022-01539-7.
- [38] R.L. Singh, P.K. Singh, R.P. Singh, Enzymatic decolorization and degradation of azo dyes – a review, Int. Biodeterior. Biodegrad. 104 (2015) 21–31, https://doi.org/ 10.1016/j.ibiod.2015.04.027.
- [39] F. Teufel, J.J. Almagro Armenteros, A.R. Johansen, M.H. Gíslason, S.I. Pihl, K. D. Tsirigos, O. Winther, S. Brunak, G. von Heijne, H. Nielsen, SignalP 6.0 predicts all five types of signal peptides using protein language models, Nat. Biotechnol. (2022), https://doi.org/10.1038/s41587-021-01156-3.
- [40] F.H. Vaillancourt, J.T. Bolin, L.D. Eltis, Ring-cleavage dioxygenases. Pseudomonas, Springer US, Boston, MA, 2004, pp. 359–395, https://doi.org/10.1007/978-1-4419-9088-4 13.
- [41] R. Vaser, I. Sović, N. Nagarajan, M. Šikić, Fast and accurate de novo genome assembly from long uncorrected reads, Genome Res. 27 (2017) 737–746, https:// doi.org/10.1101/gr.214270.116.
- [42] Y. Wang, L. Jiang, H. Shang, Q. Li, W. Zhou, Treatment of azo dye wastewater by the self-flocculating marine bacterium Aliiglaciecola lipolytica, Environ. Technol. Innov. 19 (2020) 100810, https://doi.org/10.1016/j.eti.2020.100810.
- [43] Y. Xiao, E. Zhang, J. Zhang, Y. Dai, Z. Yang, H.E.M. Christensen, J. Ulstrup, F. Zhao, Extracellular polymeric substances are transient media for microbial extracellular electron transfer, Sci. Adv. 3 (2017) 1–9, https://doi.org/10.1126/ sciadv.1700623.
- [44] X. Yu, C. Mao, S. Zong, A. Khan, W. Wang, H. Yun, P. Zhang, T. Shigaki, Y. Fang, H. Han, X. Li, Transcriptome analysis reveals self-redox mineralization mechanism of azo dyes and novel decolorizing hydrolases in Aspergillus tabacinus LZ-M, Environ. Pollut. 325 (2023) 121459, https://doi.org/10.1016/j.envpol.2023.121459.
- [45] C. Zhang, S. Wang, Y. Yan, Isomerization and biodegradation of beta-cypermethrin by Pseudomonas aeruginosa CH7 with biosurfactant production, Bioresour. Technol. 102 (2011) 7139–7146, https://doi.org/10.1016/j.biortech.2011.03.086.
- [46] S. Zhang, X. An, J. Gong, Z. Xu, L. Wang, X. Xia, Q. Zhang, Molecular response of Anoxybacillus sp. PDR2 under azo dye stress: an integrated analysis of proteomics and metabolomics, J. Hazard. Mater. 438 (2022) 129500, https://doi.org/ 10.1016/j.jhazmat.2022.129500.